

# Influence of Alloying Elements on the Glass-Forming Ability of CoFeNbBSi Alloys<sup>1</sup>

V. E. Sidorov\*, V. A. Mikhailov, and A. A. Sabirzyanov

Ural State Pedagogical University, pr. Kosmonavtov 26, Yekaterinburg, 620017 Russia

\*e-mail: sidorov@uspu.ru

Received November 12, 2015; in final form, November 28, 2015

**Abstract**—The influence of minor amounts of gallium, tin, zirconium, and antimony on the glass-forming ability of CoFeNbBSi metallic alloys is studied. The studies are performed by X-ray diffraction, transmission electronic microscopy, differential scanning calorimetry, measuring electric resistivity and magnetic susceptibility in crystalline and liquid states. Gallium and zirconium are shown to improve the glass-forming ability of the alloys whereas tin decreases it. The influence of the additions can be qualitatively described by means of the Curie paramagnetic temperature: if alloying increases it, the glass-forming ability of the alloy also increases.

DOI: 10.1134/S0036029516020166

## INTRODUCTION

Bulk metallic glasses (BMGs) are characterized by unique mechanical, magnetic, and corrosion properties. Specimens of metallic glasses several centimeters in size were formed on the basis of zirconium, titanium, and palladium [1]. In addition to these materials, which are rather aggressive at high temperatures and expensive, some compositions in bulk amorphous state were obtained on the basis of iron, cobalt, and nickel. These materials have been already implemented on a commercial scale. In particular, it was found that amorphous wires on the basis of cobalt have a giant magnetoresistance, which enabled highly sensitive detectors to be developed [2–4]. However, the wide application of cobalt bulk amorphous materials is limited by its low glass-forming ability (GFA). Hence, the problem of increasing the GFA of these alloys becomes very important.

In this work, we analyzed the influence of a small amount of gallium, tin, antimony, and zirconium on the GFA of  $\text{Co}_{47}\text{Fe}_{20.9}\text{B}_{21.2}\text{Si}_{4.6}\text{Nb}_{6.3}$  and  $\text{Co}_{48}\text{Fe}_{25}\text{B}_{19}\text{Si}_4\text{Nb}_4$  alloys. These base compositions have excellent soft magnetic properties in the state of metallic glass: the saturation magnetization is 0.5–0.9 T, the coercive force is 0.7–1.6 A/m, and the effective magnetic permeability reaches  $3.2 \times 10^4$  in a field of 1 A/m at a frequency of 1 kHz. In addition, these metallic glasses demonstrate high tensile stress of about 4250–4450 MPa at a plastic elongation of 0.6–1.3% [5, 6].

Alloying additions were selected among the elements that completely satisfy the criteria of increasing GFA of an alloy [7, 8]: the difference between the atomic radii of alloying element and the base component of the alloy (Co) is approximately 12%, and the Co–Ga, Co–Sn, Co–Zr, and Co–Sb systems are characterized by negative heats of mixing.

## RESULTS AND DISCUSSION

Amorphous CoFeNbBSi bulk metallic alloys were prepared by two methods. In the first series, cylindrical specimens with a diameter from 2 to 4 mm were obtained by suction casting. X-ray diffraction (XRD) studies demonstrated that, to obtain BMG on the basis of cobalt by vacuum suction of a melt, it is necessary to meet the following requirements: deep vacuum is not required, it is sufficiently to wash an alloy by argon, and a melt should not be highly overheated (according to DSC data, the liquidus temperature is near 1160°C; therefore, a melt should be heated to 1200–1250°C). The second series of specimens was formed by melt injection into a water-cooled copper mold. It was found that the degree of amorphization of the specimens strongly depended on the injection parameters. In particular, the melt temperature before quenching should be not lower than 1360°C, and excess pressure  $\Delta p$  should be in the range 300–340 mbar. It should be noted that the second procedure of production of BMG on the basis of cobalt turned to be more preferred: at least, the number of  $(\text{Fe, Co})_{23}\text{B}_6$  surface crystals in this case was much smaller than on the specimens produced by suction casting (Fig. 1).

<sup>1</sup> Articles presented on 14 Russian conference “Structure and Properties of Metal and Slag Melts” (MISHR-14, September 21–25, 2015, Yekaterinburg).

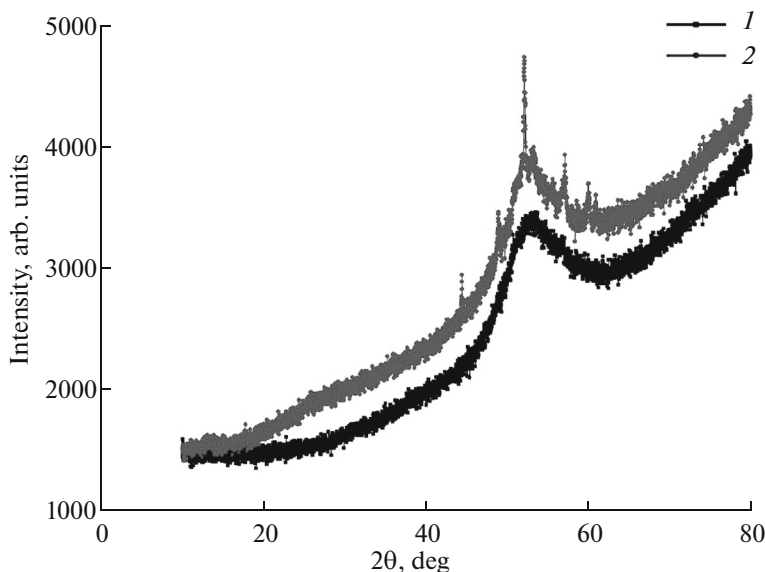


**Fig. 1.** X-ray diffraction patterns of  $\text{Co}_{48}\text{Fe}_{25}\text{B}_{19}\text{Si}_4\text{Nb}_4$  specimens 1.5 mm in diameter formed by (1) alloy injection and (2) vacuum suction.

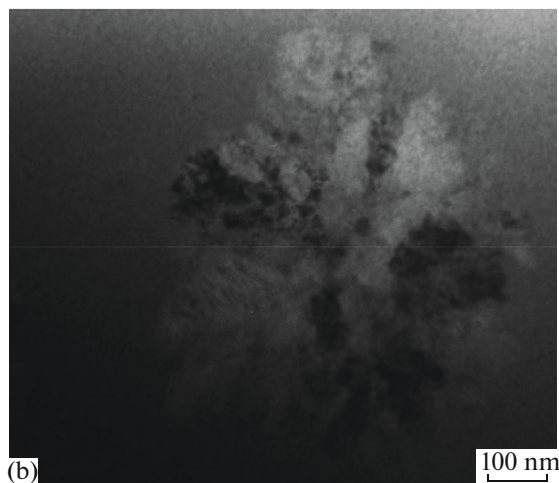
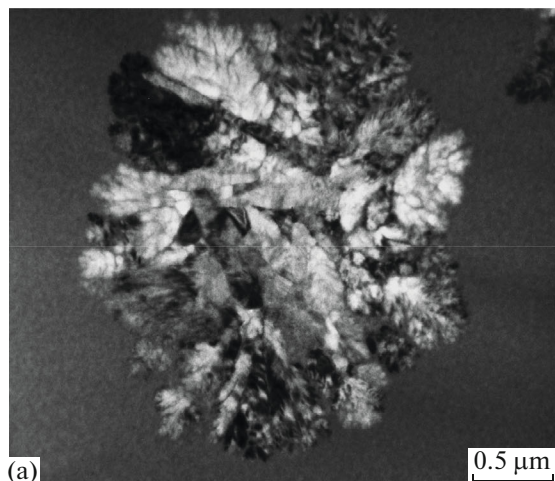


**Fig. 2.** TEM image of the central area in specimens 4 mm in diameter: (a)  $\text{Co}_{47}\text{Fe}_{20.9}\text{B}_{21.2}\text{Si}_{4.6}\text{Nb}_{6.3}$  and (b)  $[\text{Co}_{47}\text{Fe}_{20.9}\text{B}_{21.2}\text{Si}_{4.6}\text{Nb}_{6.3}]_{98}\text{Ga}_2$ .

Amorphous specimens (as determined by XRD) with a diameter of 4 mm obtained by suction casting were analyzed using a transmission electron microscope (TEM). It was found that the outer edges of the cylinders (with a thickness of about 1 mm) were completely amorphous and the central part of the cylinders contained microcrystalline inclusions. The size of these inclusions in the alloy of the base composition was 2–3  $\mu\text{m}$ . In the alloy with 2% gallium, the size of the inclusions decreased to 0.5–0.6  $\mu\text{m}$  (Fig. 2). This problem is discussed in more detail elsewhere [9, 10]. The crystalline microinclusions have a distinct dendrite structure, which makes it possible to assume that they are generated directly from the melt. In fact, these specimens were composite materials: the crystalline microinclusions were frozen into an amorphous metallic matrix.

On the basis of XRD and TEM results, it is possible to conclude that the additions of gallium and zirconium improve the GFA of  $\text{CoFeBSiNb}$  alloys, whereas the addition of tin decreases this parameter. As for antimony, we failed to obtain amorphous BMG with its addition.

To study the influence of minor additions of alloying elements on the GFA of Co-based alloys, we investigated the crystallization kinetics of these bulk amorphous alloys using a NETZSCH differential scanning calorimeter at heating rates of 5, 10, 20, and 40 K/min. Typical DSC curves are shown in Fig. 3. A glass transition temperature located by 30–40 K below the onset of crystallization is distinctly observed for all compositions. In the base alloy, crystallization occurs in one stage, whereas the additions of gallium, tin, and zirconium lead to a second stage. XRD studies revealed that the bcc  $(\text{Co}, \text{Fe})_{23}\text{B}_6$  intermetallic com-

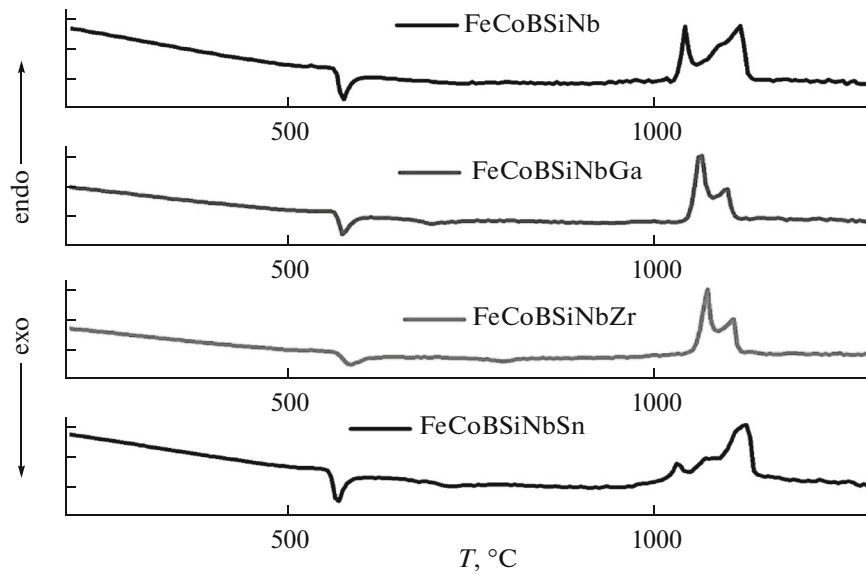


Fig. 3. DSC curves obtained for CoFeBSiNb + Ga (Sn, Zr) alloys at a heating rate of 20 K/min.

pound forms at the first stage with partial substitution of niobium atoms for cobalt atoms. At the second stage, metastable borides  $MNbB$  ( $M = Fe, Ga, Sn, Zr$ ) form; upon further heating or extended isothermal exposition, they transfer into stable compounds  $Nb_2B$  and  $Fe_2B$ . It is established that: (1) addition of 2 at % gallium decreases the glass transition temperature of  $Co_{48}Fe_{25}B_{19}Si_4Nb_4$  by 10 K and the addition of the same amount of zirconium decreases this parameter by 5 K, and the addition of tin, by 30 K; (2) additions of 2 at % gallium and zirconium weakly affects the onset of crystallization of the  $Co_{48}Fe_{25}B_{19}Si_4Nb_4$  amorphous alloy, and the addition of tin decreases it by 10 K; (3) the lowest point of the second crystallization peak is observed for the alloy with gallium, and the highest point, for the alloy with zirconium; (4) addition of gallium significantly increases the activation energy of glass formation, and the addition of tin significantly decreases this parameter; (5) addition of gallium weakly affects the activation energy of crystallization, and the addition of zirconium significantly decreases this parameter; and (6) additions of gallium

and zirconium increases the temperature of the onset of melting (solidus) of the alloy, and the addition of tin decreases this parameter.

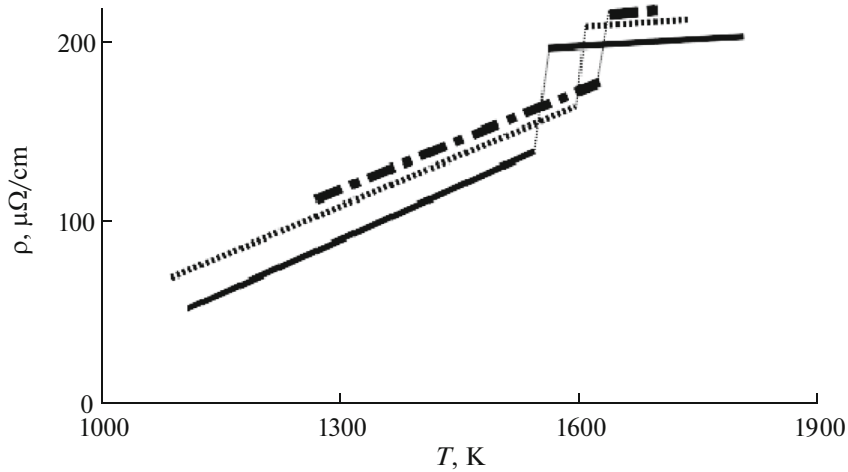
To describe the GFA of the alloys quantitatively, we calculated the most popular existing criteria of glass formation

$$\begin{aligned}
 T_{gr} &= T_g/T_m, \\
 KG &= (T_c - T_g)/(T_m - T_c), \\
 \gamma_c &= (3T_c - 2T_g)/T_m, \\
 \gamma_m &= (2T_c - T_g)/T_m, \\
 \gamma &= T_c/(T_g + T_m), \\
 \delta &= T_c/(T_m - T_g), \\
 \alpha &= T_c/T_m, \\
 \xi &= (T_c - T_g)/T_c + (T_g/T_m),
 \end{aligned}$$

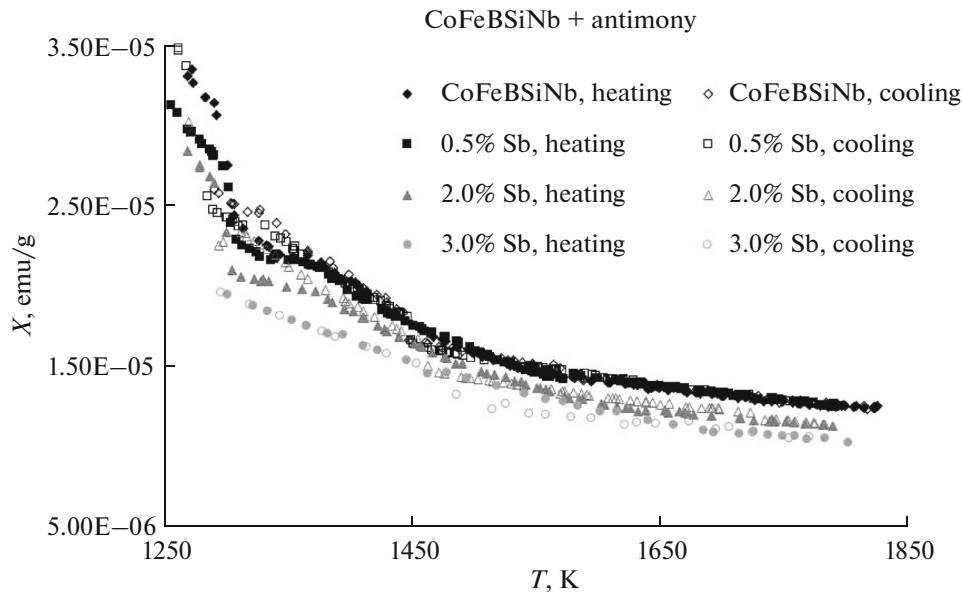
where  $T_g$  is the glass transition temperature,  $T_c$  is the crystallization point of an amorphous alloy, and  $T_m$  is the melting point (solidus). The calculation data are summarized in Table 1. It can be seen that the existing

Table 1. GFA characteristics of CoFeBSiNb alloys

Composition	$\Delta T$	$T_{gr}$	KG	$\gamma_c$	$\gamma_m$	$\gamma$	$\delta$	$\alpha$	$\xi$
FeCoBSiNb	32	0.62	0.07	0.69	0.67	0.40	1.69	0.64	0.66
FeCoBSiNbGa	47	0.60	0.10	0.71	0.67	0.40	1.60	0.64	0.66
FeCoBSiNbZr	43	0.60	0.09	0.70	0.67	0.40	1.60	0.64	0.65
FeCoBSiNbSn	53	0.61	0.12	0.73	0.69	0.40	1.65	0.65	0.67



**Fig. 4.** Temperature dependences of the electric resistivity of the alloys (solid line)  $\text{Co}_{47}\text{Fe}_{21}\text{B}_{21}\text{Si}_5\text{Nb}_6$ , (dotted line)  $[\text{Co}_{47}\text{Fe}_{21}\text{B}_{21}\text{Si}_5\text{Nb}_6]_{98}\text{Ga}_2$ , and (dot-and-dash line)  $[\text{Co}_{47}\text{Fe}_{21}\text{B}_{21}\text{Si}_5\text{Nb}_6]_{97}\text{Ga}_3$ .



**Fig. 5.** Temperature dependences of the magnetic susceptibility of CoFeBSiNb alloys with antimony.

criteria do not reflect the variation of the GFA of CoFeBSiNb alloys upon the addition of various substances, though we discovered this fact experimentally. Hence, a new criterion is required to eliminate these drawbacks, and this criterion should contain information about the melt state before quenching.

However, this problem can be solved in another way, by investigating the properties of CoFeBSiNb melts. In this work we studied the electric resistivity and the magnetic susceptibility of the alloys in crystalline and liquid states.

It was found that the electric resistivity varies linearly both in the solid and liquid states and jumps at

the liquidus point (Fig. 4). The liquidus points  $T_L$  determined from resistivity polytherms coincide with the values determined from susceptibility curves within  $\pm 3$  K. In the liquid state, resistivity as a function of temperature is described as follows:

$$\rho = \rho_0(1 + \alpha(T - T_m)),$$

where  $\rho_0$  is the electric resistivity at the liquidus point and  $\alpha$  is the temperature coefficient of resistivity (TCR). It is demonstrated that TCR weakly depends on the content of gallium in the alloy and the resistivity at the liquidus point increases from  $196 \mu\Omega \text{ cm}$  for the base composition to  $215 \mu\Omega \text{ cm}$  for the alloy with

**Table 2.** Electronic characteristics of CoFeBSiNb alloys in the liquid state

Composition	$\chi_0$ , emu/g	$N(E_F)$ , eV <sup>-1</sup>	$\theta$ , K	$C \times 10^3$ , emu K/g	$\mu_{\text{eff}}, \mu_B$
Co <sub>47</sub> Fe <sub>20.9</sub> B <sub>21.2</sub> Si <sub>4.6</sub> Nb <sub>6.3</sub>	5.88	2.2	780	6.8	1.9
[Co <sub>47</sub> Fe <sub>20.9</sub> B <sub>21.2</sub> Si <sub>4.6</sub> Nb <sub>6.3</sub> ] <sub>99.5</sub> Ga <sub>0.5</sub>	6.02	2.2	785	6.8	1.9
[Co <sub>47</sub> Fe <sub>20.9</sub> B <sub>21.2</sub> Si <sub>4.6</sub> Nb <sub>6.3</sub> ] <sub>98</sub> Ga <sub>2</sub>	4.87	1.9	815	6.8	1.9
[Co <sub>47</sub> Fe <sub>20.9</sub> B <sub>21.2</sub> Si <sub>4.6</sub> Nb <sub>6.3</sub> ] <sub>97</sub> Ga <sub>3</sub>	5.06	1.9	820	5.7	1.8
[Co <sub>47</sub> Fe <sub>20.9</sub> B <sub>21.2</sub> Si <sub>4.6</sub> Nb <sub>6.3</sub> ] <sub>99.5</sub> Sb <sub>0.5</sub>	6.01	2.3	760	6.9	1.9
[Co <sub>47</sub> Fe <sub>20.9</sub> B <sub>21.2</sub> Si <sub>4.6</sub> Nb <sub>6.3</sub> ] <sub>98</sub> Sb <sub>2</sub>	5.23	2.0	745	6.2	1.9
[Co <sub>47</sub> Fe <sub>20.9</sub> B <sub>21.2</sub> Si <sub>4.6</sub> Nb <sub>6.3</sub> ] <sub>97</sub> Sb <sub>3</sub>	4.61	1.8	715	6.3	1.8
[Co <sub>47</sub> Fe <sub>20.9</sub> B <sub>21.2</sub> Si <sub>4.6</sub> Nb <sub>6.3</sub> ] <sub>99.5</sub> Zr <sub>0.5</sub>	5.00	2.0	785	6.9	1.9

3% Ga. Assuming that gallium atoms in liquid state are in a solution, it is possible to write

$$\rho(x) = \rho_{\text{base}} + \Delta\rho,$$

where  $\rho(x)$  is the alloy resistivity,  $\rho_{\text{base}}$  is the resistivity of the base composition, and  $\Delta\rho$  is the increment due to impurity atoms. The second term can be expressed as

$$\Delta\rho = A\rho_{\text{base}}x(1-x),$$

where  $x$  is the impurity concentration and  $A$  is a normalizing constant. However, this equation is not valid in our case, since constant  $A$  depends not only on the concentration of impurity element but on temperature as well. Thus, it is possible to conclude that gallium atoms in the melt form clusters, the sizes of which decrease with increasing temperature, around them rather than existing as single pseudoatoms.

The typical polytherms of the magnetic susceptibility of CoFeBSiNb alloys at high temperatures are illustrated in Fig. 5. It should be mentioned that, on the basis of the dependence  $\chi^{-1} = f(T)$ , the liquidus point is determined accurate to  $\pm 3$  K [10]. To obtain information about the electronic structure of the alloys, the experimental dependences of their magnetic susceptibility in the liquid state were approximated by the generalized Curie–Weiss law

$$\chi(T) = \chi_0 + \frac{C}{T - \theta},$$

where  $C$  is the Curie constant,  $\theta$  is the paramagnetic Curie temperature, and  $\chi_0$  is the temperature independent contribution. On the basis of the Curie constant, it is possible to calculate the effective magnetic moment per atom in an alloy,  $\chi_0$  can be used to find the density of electron states (DOS) at the Fermi level. The calculation data are summarized in Table 2. It is established that the magnetic moment per magnetic atom in an alloy is  $1.9 \mu_B$ , which is close to the magnetic moment of cobalt atom in the liquid state. It remains constant upon the first additions of alloying elements and slightly decreases at 3 at % impurity. The DOSs at the Fermi level for the alloys are significantly

lower than for pure cobalt and iron in the liquid state. Moreover, the additions of Ga, Zr, and Sb still decrease  $N(E_F)$ . This fact evidences that the Fermi level for the alloys is at the edge of the  $3d$  band; hence, these alloys cannot be considered as good conductors. The additions of gallium and zirconium increase the paramagnetic Curie temperature, intensifying interatomic interaction in the melt, since  $\theta$  is proportional to the overlap integral between adjacent atoms. As a consequence, the additions of Ga and Zr hinder nucleation and decelerate crystal growth, which was detected in experiments. The addition of antimony decreases  $\theta$ . This means that antimony atoms are not incorporated into the existing short-range order in the melt and try to destroy it.

## CONCLUSIONS

Thus, the influence of alloying elements on the GFA of CoFeBSiNb alloys can be estimated by analyzing the magnetic susceptibility of their melts: if an addition increases the interatomic interaction in a melt (increases paramagnetic Curie temperature  $\theta$ ), it increases the GFA of the alloys; if it decreases  $\theta$ , it degrades the GFA of the alloys.

## ACKNOWLEDGMENTS

This work was supported by the Russian Foundation for Basic Research (grant no. 13-03-00598), Ministry of Education and Science of the Russian Federation (grant no. 4.1177.2014/K) and by the Government of Russian Federation (act no. 211, contract no. 02.A03.21.0006).

## REFERENCES

1. C. Suryanarayana and A. Inoue, *Bulk Metallic Glasses* (Boca Raton, CRC Press, 2011).
2. K. Mohri, K. Kawashima, and T. Kozhawa, Y. Yoshida, and L. V. Panina, "Magneto-inductive effect (MIeffect) in amorphous wires," *IEEE Trans. Magn.* **28**, 3150–3156 (1992).

3. L.V. Panina, K. Mohri, T. Uchiyama, M. Noda, and K. Bushida, "Giant magneto-impedance in Co-rich amorphous wires and films," *IEEE Trans. Magn.* **31**, 1249–1253 (1995).
4. H.Q. Guo, H. Kronmuller, T. Dragon, Z. H. Cheng, and B. G. Shen, "Influence of nanocrystallization on the evolution of domain patterns and the magnetoimpedance effect in amorphous Fe<sub>73.5</sub>Cu<sub>1</sub>Nb<sub>3</sub>Si<sub>13.5</sub>B<sub>9</sub> ribbons," *J. Appl. Phys.* **89**, 514–518 (2001).
5. Q. Man, H. Sun, Y. Dong, B. Shen, H. Kimura, A. Makino, and A. Inoue, "Enhancement of glass-forming ability of CoFeBSiNb bulk glassy alloys with excellent soft-magnetic properties and superhigh strength," *Intermetallics* **18**, 1876–1879 (2010).
6. Y. Dong, A. Wang, Q. Man, and B. Shen, "(Co<sub>1-x</sub>Fe<sub>x</sub>)<sub>68</sub>B<sub>21.9</sub>Si<sub>5.1</sub>Nb<sub>5</sub> bulk glassy alloys with high glass-forming ability, excellent soft-magnetic properties and super-high fracture strength," *Intermetallics* **23**, 63–67 (2012).
7. A. Inoue, "Stabilisation of metallic supercooled liquid and bulk amorphous alloys," *Acta Mater.* **48**, 279–306 (2000).
8. A. Inoue and A. Takeuchi, "Recent progress in bulk glassy, nanoquasicrystalline and nanocrystalline alloys," *Mater. Sci. Eng. A.* **375–377**, 16–30 (2004).
9. J. Hosko, I. Janotova, P. Svec, D. Janickovic, G. Vlasak, E. Illekova, I. Matko, and P. Sr. Svec, "Preparation of thin ribbon and bulk glassy alloys in CoFeBSiNb(Ga) using planar flow casting and suction casting methods," *J. Non-Cryst. Solids.* **358**, 1545–1549 (2012).
10. V. Sidorov, J. Hosko, V. Mikhailov, I. Rozkov, N. Uporova, P. Svec, D. Janickovic, I. Matko, P. Sr. Svec, and L. Malyshev, "Magnetic susceptibility of CoFeBSiNb alloys in liquid state," *J. Magn. Magn. Mater.* **354**, 35–38 (2014).

*Translated by I. Moshkin*